Pol. J. Environ. Stud. Vol. 31, No. 6 (2022), 5057-5070
DOI: *10.15244/pjoes/151112* ONLINE PUBLICATION DATE: 2022-09-12

Original Research

Comparative Study on Emission Reduction Performance of Inorganic Acid and Organic Acid Rare Earth Fuel Additives for Diesel Engines

Guo Junwu*, Guo Leyang

Shanghai Maritime University, Marine Merchant College, No.1550 Haigang Avenue, Shanghai, China

Received: 4 May 2022
Accepted: 18 June 2022

Abstract

Among existing diesel engines, fuel improvement through additives is an attractive option to meet increasingly stringent pollutant emission regulations for diesel engines. Because of the good REDOX properties of rare earth materials, it can improve the combustion performance of diesel engines and reduce pollutant emissions. This paper characterizes the performance of inorganic acid rare earth and organic acid rare earth and analyzes the emission reduction performance from the crystal structure, which aim to compare the effects of inorganic acid rare earth and organic acid rare earth on the emission reduction performance of existing diesel engines under similar conditions. The emission reduction performance of two rare earth fuel additives of cerium carbonate and cerium stearate in Changchai twin-cylinder direct injection diesel engine at five rotational speeds is contrastively studied. The experimental results show that two kinds of rare earth fuel additives can effectively reduce NO_X, CO and HC emissions of diesel engines. And the maximum reduction rate of NO_X, CO and HC in cerium carbonate is 11.37%, 14.63% and 13.80% respectively, while the maximum reduction rate of NO_X, CO and HC in cerium stearate is 10.19%, 12.15% and 9.40% respectively. Cerium stearate has higher NO_X, CO, HC and PM emissions than cerium carbonate due to its small specific surface area. So the emission reduction effect of cerium carbonate is better than that of cerium stearate.

Keywords: inorganic acid, organic acid, rare earth, emission reduction

Introduction

Fuel additives can effectively improve the combustion performance of diesel engines to reduce emissions, and fuel additives have the characteristics of low investment, no additional equipment, no change in diesel engine structure, easy operation and good effect. Therefore, the use of fuel additives has become one of the main research directions of diesel engine emission reduction.

Prelec Z. et al. [1] have conducted the research during real operating conditions of a steam boiler, belonging to a 320 MW power plant, in order to reveal fuel additive effectiveness in controlling flue gas emissions, plant availability, maintenance costs and operating efficiency.

In this study of Benk A. et al. [2], the production of fuel and fuel additives from low-viscosity waste renewable mineral oils, called number-10 oil in Turkey, and also of their mixtures, was investigated in detail.

*e-mail: jwguo@shmtu.edu.cn

Preparation and utilization method of a new Fe-nanofluid based heavy fuel oil additive for particulate matter reduction in heavy fuel oil fired boiler facilities have been presented and discussed. [3]

Tumanyan B.P. et al. [4] studied the use of vegetable-oil fatty acids as lubricity additives for modern diesel fuels with ultra-low sulfur contents.

Pretreatment of the crude oil with flow improver or pour point depressants has received the greatest acceptance due to its simplicity and economy. Four commercial additives were evaluated as pour point depressant for fuel oils. The structures of the commercial additives were confirmed by FTIR spectra [5].

Shah P.R. [6] intended to compare the behaviour of edible and non-edible crude vegetable oil on engine characteristics of existing diesel engine under similar operating condition with cognitive elaboration.

The world situation in the field of additives that provide for the manufacture of standard fuels at oil refineries has been considered by Danilov, AM [7].

Jang Sh. et al. [8] investigated the effects of fuel additives, not only at the scale of the engine test bed but also through chemical laboratory tests. Fuel separability tests were conducted to evaluate fuel oil stability.

WO_3 was used as fuel additive in diesel oil. Fire and flash points of diesel oil were enhanced to 49 degrees C and 54 degrees C respectively. The calorific value was increased up to 36580. Thus fuel efficiency was enhanced by use of WO_3 as an additive [9].

Research on the potency of essential oils as diesel fuel bio-additives has been reported. It also has been found out that clove oil has a better performance than turpentine oil on decreasing Break Specific Fuel Consumption and reduces the exhaust emissions of the engine [10].

Experimental data on frequency-temperature relationships tan delta (t, f) for diesel fuel and the diesel containing the pour-point depressant Dodiflow-4971 and C-10-C-18 higher fatty alcohols are presented [11].

Comparative study of fatty acids isolated from vegetable (sunflower and cotton-seed) oils and tall oil fatty acids was carried out as regards the possibility of their application as raw material for production of anti-wear additives to low-sulfur diesel fuels [12].

The introduction into diesel fuel of cottonseed oil additives and methanol etherification products was studied. The change occurring in the physical-chemical and operational properties of diesel fuel as a result of the introduction of these additives was determined. The optimal additions of cottonseed oil and mixtures of its ethers in diesel fuel were recommended [13].

Based on the analysis of literature and patent information, the situation pertaining to fuel additives in the period 2006-2010 was reviewed. The major trends in additive development were shown and the main types of additives were characterized [14].

The effects of reaction temperature and catalyst additives on the fluid catalytic cracking products yield have been studied through cracking of a heavy fuel oil obtained from Tehran refinery [15].

In this study, the effects of industrial polymer additives and surfactants that are economically acceptable on decrement of pour point temperature were studied by using three oil product samples, namely light diesel, heavy diesel, and fuel oil. Furthermore, optimized type and concentration of the additives were studied [16].

This paper investigates the friction reducing properties and fuel saving potential of a boric acid based fuel additive with remarkably promising results in field tests [17].

This review covered the recent reports related to the recent developments in the field of application of various types of fuel additives for reduction of particulate matter/dust in exhaust gases resulting from incomplete combustion of hydrocarbon fuels [18].

The present study intended to explore the effect of the addition of fuel additives with camphor oil on the characteristics of a twin-cylinder compression ignition engine [19].

In this study, two fuel additives, oil-soluble Ca-based and oil-soluble Fe-based organometallic compounds, which could improve the performance of diesel engines, were injected into HFO at fixed concentrations (1/4000 and 1/6000 of the total fuel, respectively), in attempts to reduce fuel consumption and exhaust emissions [20].

Multifunctional diesel fuel additives SOMAN and SO-2E were obtained on the basis of kukersite shale oil fractions. Possibilities for the practical application of the additives in diesel engines under actual service conditions were considered [21].

This paper investigated the effects of anisole and methyl acetate (as fuel additives) on the performance and emission characteristics of a compression-ignition diesel engine [22].

The situation evolved in the domain of fuel additives production during 2011-2015 was reviewed through the analysis of literature and patent sources and statistical data. The main trends in development of additives were determined and the main types of additives were characterized. It was noted that the interest of developers worldwide was focused on additives of biocomponents (oxygenates and biodiesel) [23].

The objective of Aynaz M. et al. [24] was to compare the adsorption efficiency of two types of magnetic activated carbons derived from Banana peel and Salvia seed for the removal of basic blue 41 dye.

Razieh K. et al. [25] provided further evidence for the significant effect of monoxide carbon on asthma; and suggested that temperature might have a role in the exacerbation of asthma.

Reza S. et al. [26] conducted to evaluate ciprofloxacin (CIP) adsorption efficiency onto the multi-walled carbon nanotube (MWCNTs) and magnetic multi-walled carbon nanotube (MMWCNTs).

Abdollah D. et al. [27] designed the experiments based on the central composite design (CCD) and

analyzed and modeled by response surface methodology (RSM) to demonstrate the operational variables and the interactive effect of four independent variables on two responses.

From the above references, we can know that fuel additives are widely used, however there is little research on rare earth fuel additives. In particular, there are no studies comparing the emission reduction performance of inorganic acid rare earth and organic acid rare earth. At present, both organic acid rare earth and inorganic acid rare earth can be applied to diesel engine emission reduction. In order to study the effect of inorganic acid rare earth and organic acid rare earth fuel additives on diesel engine emission reduction, cerium carbonate and cerium stearate are selected for comparative study. The novelty and purpose of the research in this paper is to compare the emission reduction performance of cerium carbonate and cerium stearate, and finally, it is concluded that cerium carbonate has the best emission reduction performance.

Material and Methods

Preparation of Cerium Carbonate

The advantages of the preparation method of cerium carbonate in this paper are simple and easy to operate, no drying products and stabling product quality. The specific preparation process is as follows:

A cerium chloride ($CeCl_3$) is heated to 100 degrees Celsius and stabilized, its concentration is 50-90 g/L. The cerium solution is continuously stirred with a magnetic stirring rod, and ammonium bicarbonate solution (NH_4HCO_3) is added to the cerium solution at a steady and slow speed until the PH value of the mixed solution is stabilized about 6.4, then adding NH_4HCO_3 stops. The mass ratio of CeO_2: NH_4HCO_3 in the mixed solution is 2:3. The mixed solution passes through the precipitation stage, filtration stage, continuous washing and centrifugal drying stage to obtain light yellow crystal. The crystal is the prepared cerium carbonate with the molecular formula $Ce_2(CO_3)_3$. Its chemical reaction principle is as follows:

$$2CeCl_3 + 6NH_4HCO_3 = Ce_2(CO_3)_3 + 6NH_4Cl + 3CO_2 + 3H_2O \quad (1)$$

Performance Characterization of Cerium Carbonate

In this paper, a scanning electron microscope (S-4800) manufactured by Hitachi Co., LTD. in Japan is used, which can be used not only as a scanning electron microscope, but also for X-ray energy spectrum analysis.

Scanning Electron Microscopy (SEM)

The prepared cerium carbonate was centrifugically dried and then analyzed by SEM, as shown in Fig. 1.

SEM images show that the size of cerium carbonate particles is 5-10 μm, most of the particles are discrete, no obvious particle agglomeration, the distance between the particles is large and the gap is obvious.

From the low-magnification SEM images of 1 K and 5 K, it can be seen that the morphology of cerium carbonate is massive, and the particles can gather together, and there is a certain agglomeration phenomenon, it indicates that the centrifugal drying process is not complete.

It can be seen from the high-magnification SEM images of 10 K and 30 K that there are many gaps between the fine particles of cerium carbonate, which

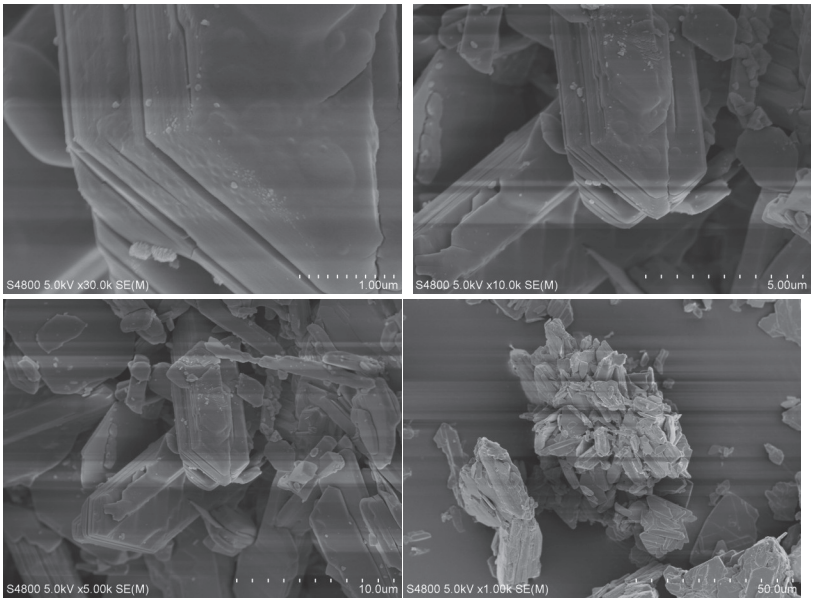

Fig. 1. SEM image of cerium carbonate.

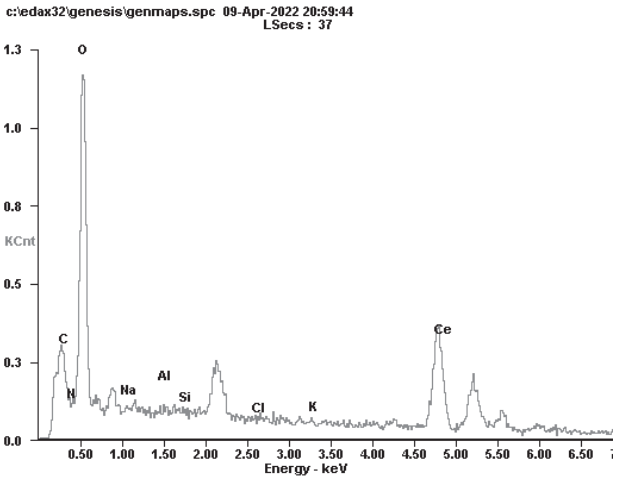

Fig. 2. EDS energy spectrum of cerium carbonate.

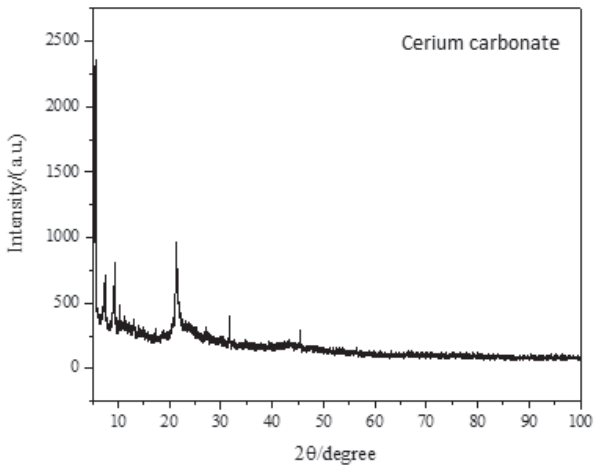

Fig. 3. X-ray diffraction analysis of cerium carbonate.

Table 1. Contents of elements in cerium carbonate.

Element	Wt %	At %
CK	12.03	32.24
OK	21.14	42.54
CeL	61.78	14.19
Matrix	Correction	ZAF

are conducive to increasing the specific surface area and easy to fully mix and contact with diesel oil.

Analysis of X-ray Energy Disperse Spectroscopy (EDS)

EDS analysis of cerium carbonate powder is shown in Fig. 2. In the figure, the ordinate is the count rate CPS of X-ray photons, and the abscissa is the energy value KeV of elements.

Fig. 2 and Table 1 show that the prepared cerium carbonate powder is mainly composed of cerium, carbon and oxygen elements. There is no hydrogen element and no other impurity element in the test. The weight ratio and atomic number ratio of cerium are 61.78% and 14.19% respectively. Compared with the chemical formula, the proportion of O and C elements are less, the possible reason is that the preparation reaction process is not thorough enough.

X-ray Diffraction Analysis (XRD)

The X-ray diffractometer used in this paper is X ‘Pert3 Powder, which is manufactured by PANnlytical Co., LTD. in Netherlands. XRD analysis results of cerium carbonate powder are shown in Fig. 3. Compared with the standard card number 00-043-1002, it is found that although there is no obvious miscellaneous peak in Fig. 3, there is still a certain small intensity diffraction peak, because the PH value is not stable enough at 6.4 during the preparation process, and certain miscellaneous phase appears. But the purity is greater than 95%, so the preparation is successful.

Specific Surface Area Analysis (BET)

The specific surface physical adsorption instrument used in this paper is ASAP 2020M, which is an automatic specific surface and micropore pore size analyzer manufactured by Micrometric LTD in USA. The nitrogen adsorption isotherms of cerium carbonate can be obtained by drawing the nitrogen adsorption capacity Va and the relative pressure P/P0, as shown in Fig. 4. As can be seen from Fig. 4, with the increase of relative pressure, adsorption capacity of cerium carbonate rises steadily, but the rising levels off, the rising velocity is declining. When the adsorption equilibrium pressure is close to saturation pressure (0.9373 p/p°), the greater the relative pressure is, the adsorption capacity is the rapid increase trend, as high as 58 cm^3/g, it shows the multilayer adsorption phenomenon.

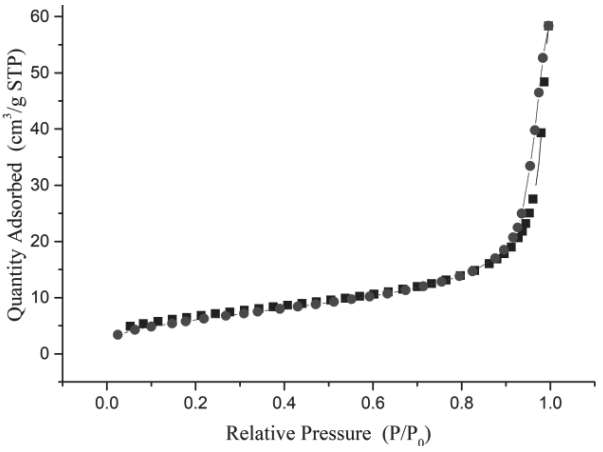

Fig. 4. Isothermal adsorption curve of cerium carbonate.

Through automatic analysis of specific surface area instrument, it can be known that the specific surface area of cerium carbonate powder is 23.7525 m²/g, and the average pore size between powder particles is 15.0728 nm, so its specific surface area is large.

Preparation of Cerium Stearate

Cerium stearate is synthesized by direct method.

A wash and dry 500 ml wild-mouth bottle is taken to prepare a certain concentration of cerium nitrate solution, specific steps are as follows: a certain amount of cerium oxide are taken into wild-mouth bottle, the right amount of nitric acid solution are poured into wild-mouth bottle, cerium oxide dissolves slowly by heating, the heating finishes after the solution is clarified, the cerium nitrate solution is diluted to the corresponding mass concentration with distilled water.

Then taking a wash and dry conical bottle, amount of stearic acid and the appropriate number of ethanol as solvent are added into conical bottle, the solution is stirred under the condition of heating until stearic acid is completely dissolved. Then stearic acid solution is heated to a certain temperature and stirred, and the cerium nitrate solution is slowly dripped into the stearic acid solution and stands for a certain period of time. After stirring well, proper amount of sodium hydroxide solution are added to adjust PH to neutral and stability. After adding, then the solution temperature is kept for a period of time to filter the solution. After filtering and cooling the solution, final precipitate is a white powder which is the cerium stearate. The cerium stearate powder is washed and dried to constant weight, its molecular formula is $Ce(C_{18}H_{35}O_2)_3$. Its chemical reaction principle is as follows:

$$3C_{18}H_{36}O_2 + Ce(NO_3)_3 = Ce(C_{18}H_{35}O_2)_3 + 3HNO_3 \quad (2)$$

Performance Characterization of Cerium Stearate

Analysis of Scanning Electron Microscopy (SEM)

The prepared cerium stearate powder is centrifugically dried and then analyzed by SEM, as shown in Fig. 5. As can be seen from Fig. 5, the particle size of cerium stearate is irregular, round-like and massive particles. The monolayer particles are uniformly distributed, and most of the particles do not agglomerate obviously. Due to the incomplete centrifugal drying in the preparation, slight crystal accumulation may result in rough surface of the particles.

In general, the crystal size varies very little, the particle size reaches the nanometer scale. Although the particles have irregular arrangement and shape, the good dispersion indicates that the cooling crystallization effect is good in the preparation process. It can be observed from the high magnification image that the particle surface is not smooth and the crystal intensity is high, but the remaining distance between the crystals is still large, and some particles have a few pores on the surface.

Analysis of X-ray Energy Disperse Spectroscopy (EDS)

EDS analysis of cerium stearate powder is shown in Fig. 6. In the figure, the ordinate is the count rate CPS of X-ray photons, and the abscissa is the energy value KeV of elements.

As can be seen from Fig. 6 and Table 2, cerium stearate powder is mainly composed of cerium, carbon and oxygen. The weight and atomic number percentage of cerium element are 23.35% and 2.72% respectively. The atomic number of cerium element accounts for

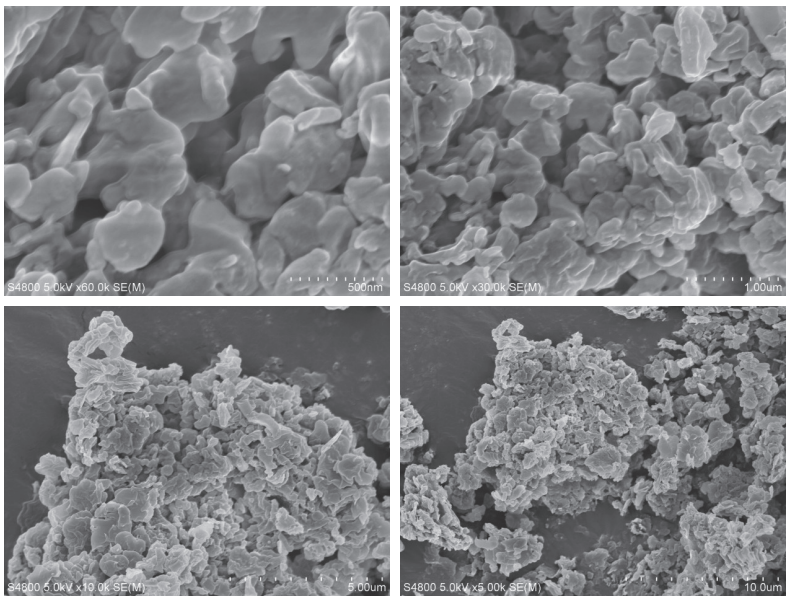

Fig. 5. SEM image of cerium stearate.

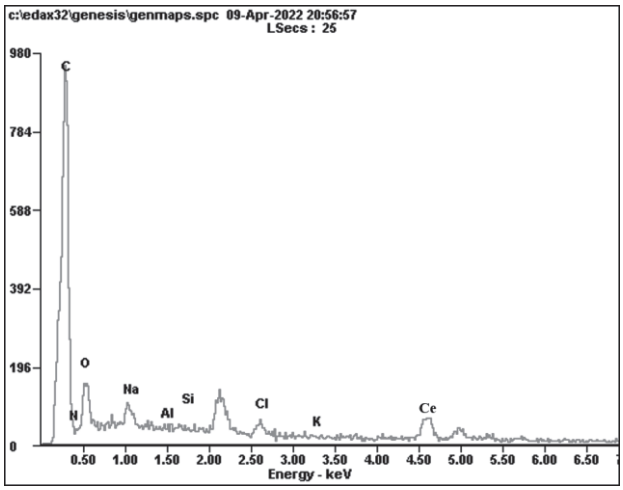

Fig. 6. EDS spectrum of cerium stearate.

Table 2. Contents of elements in cerium stearate.

Element	Wt %	At %
CK	61.36	82.66
NK	03.79	04.38
OK	08.13	08.22
CeL	23.35	02.72
Matrix	Correction	ZAF

a relatively high proportion due to the incomplete reaction in the preparation process.

X-ray Diffraction Analysis (XRD)

XRD analysis results of cerium stearate powder are shown in Fig. 7.

Fig. 7 is compared with standard card number 00-083-1211, it is found that no obvious impurity peak

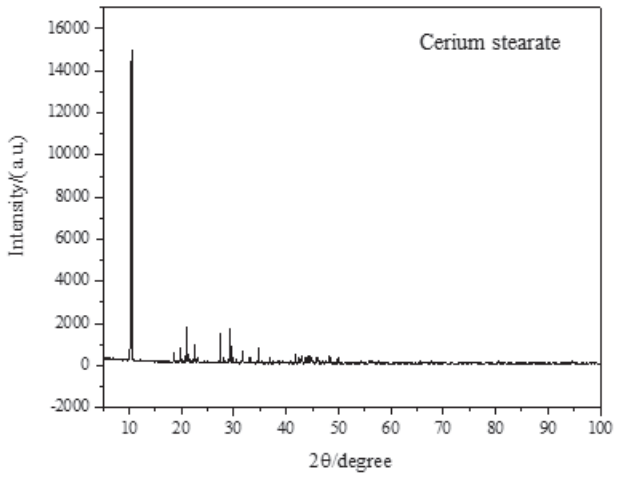

Fig. 7. X-ray diffraction analysis of cerium stearate.

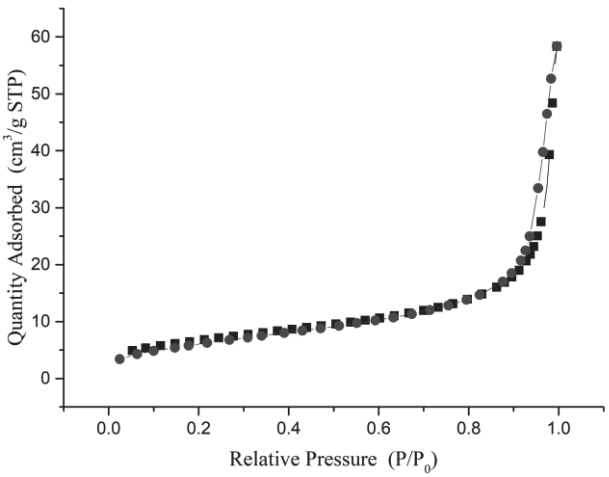

Fig. 8. Isothermal adsorption curve of cerium stearate.

and diffraction peak width phenomenon appeared, so the characteristics of the cerium stearate is significant without dispersion diffraction peak. However, there is a diffraction peak of small intensity, indicating that there may be impurity elements in the preparation process. Combined with EDS analysis, it is found that the additive cerium nitrate solution is too much.

Specific Surface Area Analysis (BET)

The nitrogen adsorption isotherms for cerium stearate can be obtained by drawing the nitrogen adsorption capacity Va against the relative pressure P/P_0, as shown in Fig. 8. It can be seen from the Fig. 8 that the adsorption capacity of cerium stearate increases steadily with the increase of relative pressure. When the adsorption equilibrium pressure is close to the saturation pressure (0.9531 P/P°), the adsorption capacity shows a trend of rapid increase, up to 53.09 cm^3/g, it shows multilayer adsorption phenomenon. A comparison of Fig. 4 and Fig. 8 shows that the rate of cerium stearate is faster than cerium carbonate.

The specific surface area of cerium stearate powder is 11.7797 m^2/g, and the average pore size between powder particles was 32.9169 nm. Compared with cerium carbonate powder, the specific surface area of cerium stearate powder is smaller than cerium carbonate powder, and the average pore size between particles is larger than cerium carbonate powder.

Results and Discussion

Establishment of Diesel Engine Experimental Platform

After analyzing the characteristics of cerium carbonate and cerium stearate, the emission reduction performance of cerium stearate and cerium carbonate

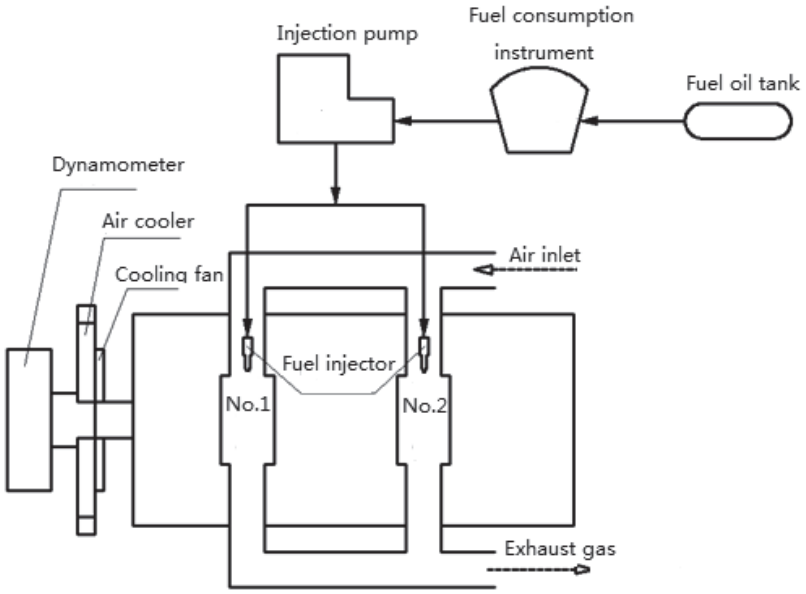

Fig. 9. Schematic diagram of experimental platform.

as diesel engine fuel additives must be verified on the diesel engine experimental platform. A diesel engine experimental platform is built to meet the test requirements, and its schematic diagram is shown in Fig. 9.

The diesel engine used for the experimental platform is Changchai CZ2102 diesel engine, whose technical number is shown in Table 3. Changchai CZ2102 diesel engine experimental platform is shown in Fig. 10.

Table 3. Parameters of Changchai CZ2102 diesel engine.

Item	Parameters
Type	CZ2102
Series	102
Number of cylinders	2
Cylinder diameter × stroke	102 mm×118 mm
Total emissions	1.928 L
Air intake form	Naturally aspirated
Cylinder arrangement	Inline
Injection way	Direct injection
Cooling way	Water cooled
Maximum output power	29 kw
Rated speed	2800 rpm
Net weight	215 kg
Emission standards	Country 2 / Euro 2
Diesel engine size	550×580×730 mm
Maximum horsepower	40 horsepower

Exhaust gas component of diesel engine is tested by a third party testing institutions for laboratory testing. Third party testing institutions is Shanghai Fudan Testing Technology Group Co., Ltd. The laboratory analysis equipment mainly consists of a gas chromatograph, which model is Agilent 7890B, the hydrogen flame ionization detector (FID), thermal conductivity detector (TCD), 5977B mass spectrometer detector, and gas mass spectrometer, which model is Dycor LC-D Series.

Emission Reduction Experiment of Cerium Carbonate Additives

$0^{\#}$ diesel oil is taken as the reference group, which is denoted as F0. Cerium carbonate is added into $0^{\#}$ diesel oil to make the mass fractions reach 20 mg/L, 40 mg/L, 60 mg/L and 80 mg/L, which are marked as experimental groups C20, C40, C60 and C80

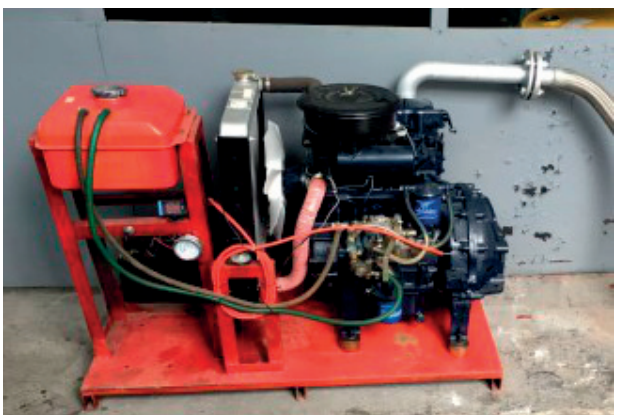

Fig. 10. Experimental platform of Changchai CZ2102 diesel engine.

respectively. The diesel engine is tested at the rated speed of 60%, 70%, 80%, 90% and 100% respectively, and the exhaust emission value is measured after 15 minutes of stable operation. The exhaust emission value should be measured five times to get the average value. The specific measurement data are shown in Figs 11, 12, 13, 14 and Table 4, 5, 6, 7.

As can be seen from Fig. 11 and Table 4, with the increase of diesel engine speed, the nitrogen oxide concentration discharged presents an increasing trend. After comparative analysis, the NO_X emission reduction effect increases with the increase of the mass fraction of additives. The maximum reduction of NO_X concentration is 11.37%.

As can be seen from Fig. 12 and Table 5, with the increase of diesel engine speed, the CO concentration discharged presents a downward trend. However, when the speed exceeds 90% of rated speed, CO emission concentration has a little upward trend. After comparative analysis, CO emission reduction effect also increases with the increase of the mass fraction of additives, and the maximum reduction of CO concentration is 14.63%.

As can be seen from Fig. 13 and Table 6, with the increase of diesel engine speed, HC concentration discharged presents a downward trend. After comparative analysis, HC emission reduction effect also increases with the increase of the mass fraction of additives, and the maximum reduction of HC concentration is 13.80%.

As can be seen from Fig. 14 and Table 7, with the increase of diesel engine speed, the exhaust PM concentration shows an upward trend. After comparative analysis, the increase rate of PM emission increases with the increase of the mass fraction of additives, and the maximum increase of PM concentration is 10.86%.

It can be seen that cerium carbonate powder is analyzed by BET, SEM, XRD and EDS, and more comprehensive characterization data are obtained through the performance characterization. SEM images show that cerium carbonate has massive morphology, which may be caused by artificial errors of incomplete centrifugal drying, resulting in loose sample structure and certain agglomeration phenomenon. However, there are many particle gaps and

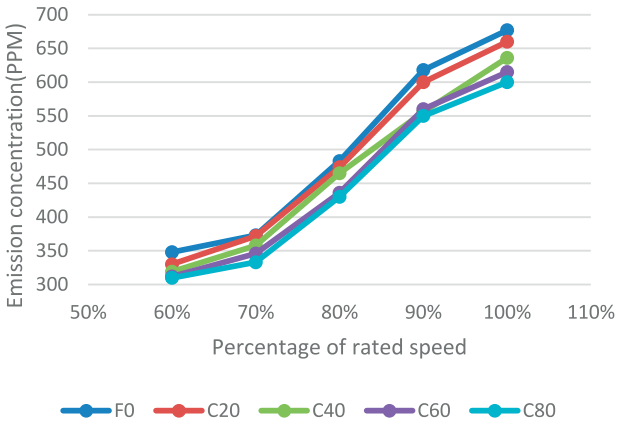

Fig. 11. Broken line chart of NO_X emission concentration of cerium carbonate additives.

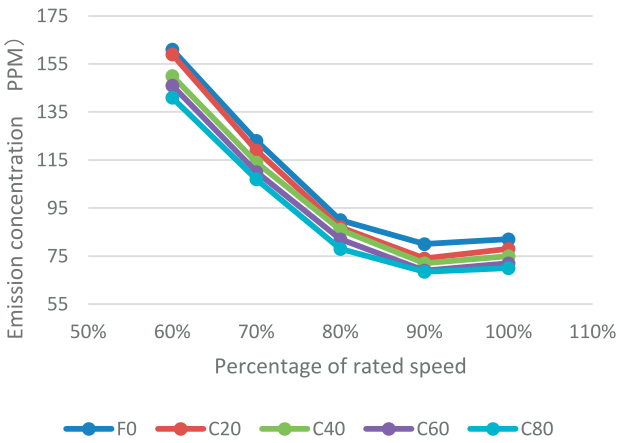

Fig. 12. Broken line chart of CO emission concentration of cerium carbonate additives.

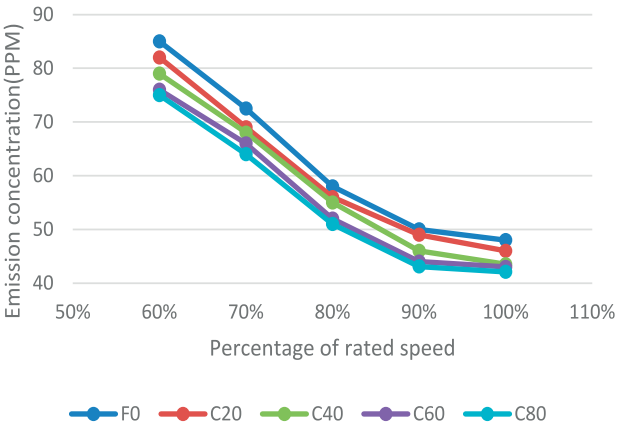

Fig. 13. Broken line chart of HC emission concentration of cerium carbonate additives.

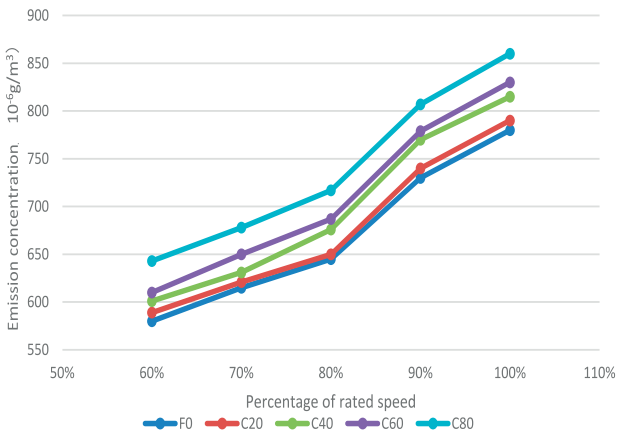

Fig. 14. Broken line chart of PM emission concentration of cerium carbonate additives.

large specific surface area, which is easy to mix with fuel. The weight and atomic number percentage of cerium element are 61.78% and 14.19%, respectively. Therefore, cerium carbonate powder is suitable for additive. After calculation and analysis, the specific surface area of cerium carbonate powder is 23.7525 m²/g, and the average pore size between powder particles is 15.0728 nm. Good emission reduction effect was obtained on the experimental platform, it is concluded that the emission concentration of NO_X, CO and HC decreases by 11.37%, 14.63% and 13.8% respectively, but the maximum increase of PM particle concentration is 10.86%. Therefore, compared with 0# diesel alone, cerium carbonate fuel additive has better pollution reduction effect comprehensively.

Emission Reduction Experiment of Cerium Stearate Additives

$0^{\#}$ diesel oil is taken as the reference group, it is denoted as F0. Cerium stearate is added into $0^{\#}$ diesel oil to make the mass fractions reach 20 mg/L, 40 mg/L, 60 mg/L and 80 mg/L respectively, which are marked as experimental groups S20, S40, S60 and S80 respectively. The diesel engine is tested at the rated speed of 60%, 70%, 80%, 90% and 100% respectively, and the exhaust emission value is measured after 15

Table 4. NO_X emission concentration of cerium carbonate additives.

RPM	F0	C20		C40		C60		C80		Average decline	Error (%)
	NO_X	NO_X	Decrement	NO_X	Decrement	NO_X	Decrement	NO_X	Decrement		
60%	348	330	5.17	319	8.33	312	10.34	310	10.92	8.69	1.2
70%	373	372	0.27	358	4.02	346	7.24	333	10.72	5.56	2.5
80%	483	474	1.86	465	3.73	436	9.73	430	10.97	6.57	1.1
90%	618	600	2.91	556	10.03	560	9.39	550	11.00	8.33	1.3
100%	677	660	2.51	636	6.06	615	9.16	600	11.37	7.28	1.4
Average			2.54		6.43		9.17		11.00	7.29	1.5

Table 5. CO emission concentration of cerium carbonate additives.

RPM	F0	C20		C40		C60		C80		Average decline	Error (%)
	CO	CO	Decrement	CO	Decrement	CO		CO	Decrement		
60%	161	159	1.24	150	6.83	146	9.32	141	12.42	7.45	2.4
70%	123	119	3.25	114	7.32	110	10.57	107	13.01	8.54	1.2
80%	90	87	3.33	86	4.44	82	8.89	78	13.33	7.50	1.3
90%	80	74	7.50	72	10.00	69	13.75	68.5	14.38	11.41	1.1
100%	82	78	4.88	75	8.54	72	12.20	70	14.63	10.06	1.0
Average			4.04		7.43		10.95		13.55	8.99	1.4

Table 6. HC emission concentration of cerium carbonate additives.

RPM	F0	C20		C40		C60		C80		Average decline	Error (%)
	HC	HC	Decrement	HC	Decrement	HC	Decrement	HC	Decrement		
60%	85	82	3.53	79	7.06	76	10.59	75	11.76	8.24	1.1
70%	72.5	69	4.83	68	6.21	66	8.97	64	11.72	7.93	1.2
80%	58	56	3.45	55	5.17	52	10.34	51	12.07	7.76	1.3
90%	50	49	2.00	46	8.00	44	12.00	43.1	13.80	8.95	1.0
100%	48	46	4.17	43.5	9.38	43	10.41	42.1	12.29	9.06	2.4
Average			3.60		7.16		10.46		12.33	8.39	1.4

Table 7. PM emission concentration of cerium carbonate additives.

RPM	F0	C20		C40		C60		C80		Average growth	Error (%)
	PM	PM	Growth	PM	Growth	PM	Growth	PM	Growth		
60%	580	589	1.55	601	3.60	610	5.17	643	10.86	5.30	1.6
70%	615	621	0.98	631	2.60	650	5.69	678	10.24	4.88	1.2
80%	645	650	0.78	676	4.81	687	6.51	717	11.16	5.82	1.7
90%	730	740	1.37	770	5.48	779	6.71	807	10.55	6.03	1.4
100%	780	790	1.28	815	4.49	830	6.41	860	10.26	5.61	1.3
Average			1.19		4.20		6.10		10.61	5.53	1.4

minutes of stable operation. The exhaust emission value should be measured five times to get the average value. The specific measurement data is shown in Figs 15, 16, 17, 18 and Table 8, 9, 10, 11.

As can be seen from Fig. 15 and Table 8, with the increase of diesel engine speed, the nitrogen oxide concentration discharged presents an increasing trend. After comparative analysis, the NO_X emission reduction effect increases with the increase of the mass fraction of additives. The maximum reduction of NO_X concentration is 10.19%.

As can be seen from Fig. 16 and Table 9, with the increase of diesel engine speed, the CO concentration discharged presents a downward trend. However, when the speed exceeds 90% of rated speed, CO emission concentration has a little upward trend. After comparative analysis, CO emission reduction effect also increases with the increase of the mass fraction of

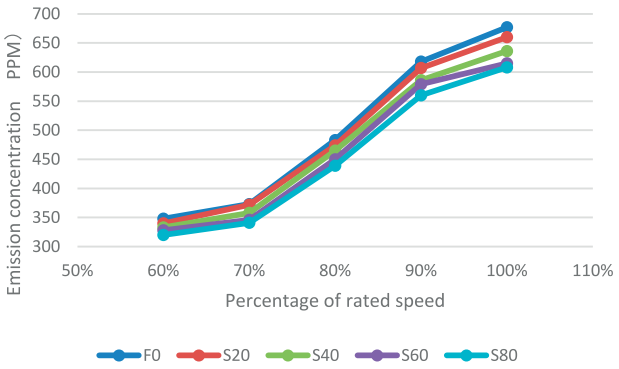

Fig. 15. Broken line chart of NO_X emission concentration of cerium stearate additives.

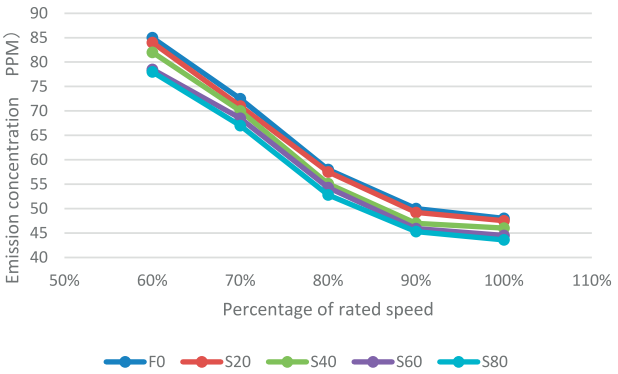

Fig. 17. Broken line chart of HC emission concentration of cerium stearate additives.

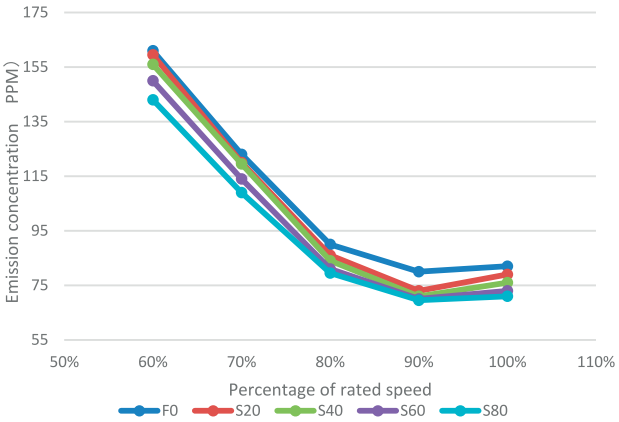

Fig. 16. Broken line chart of CO emission concentration of cerium stearate additives.

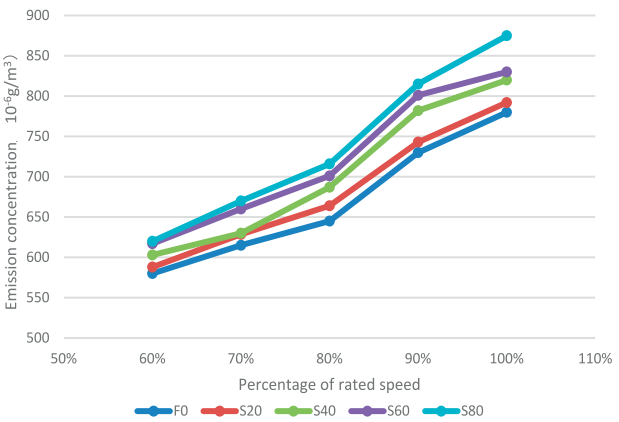

Fig. 18. Broken line chart of PM emission concentration of cerium stearate additives.

Table 8. NO_X emission concentration of cerium stearate additives.

RPM	F0	S20		S40		S60		S80		Average decline	Error (%)
	NO_X	NO_X	Decrement	NO_X	Decrement	NO_X	Decrement	NO_X	Decrement		
60%	348	340	2.30	333	4.31	328	5.75	320	8.05	5.10	2.2
70%	373	372	0.27	358	4.02	346	7.24	341	8.58	5.03	1.5
80%	483	474	1.86	465	3.73	450	6.83	439	9.11	5.38	1.4
90%	618	607	1.78	586	5.18	579	6.31	560	9.39	5.67	1.3
100%	677	660	2.51	636	6.06	615	9.16	608	10.19	6.98	1.2
Average			1.74		4.66		7.06		9.06	5.63	1.5

Table 9. CO emission concentration of cerium stearate additives.

RPM	F0	S20		S40		S60		S80		Average decline	Error (%)
	CO	CO	Decrement	CO	Decrement	CO	Decrement	CO	Decrement		
60%	161	159.5	0.93	156	3.11	150	6.83	143	11.18	5.51	1.2
70%	123	120	2.44	119.5	2.85	114	7.32	109	11.38	5.60	1.4
80%	90	86	4.44	84	6.67	81	10.00	79.5	11.67	8.20	1.1
90%	80	73	8.75	71	11.25	70	8.75	69.5	13.13	10.47	2.8
100%	82	79	3.66	76	7.32	73	10.98	71	13.41	8.84	1.3
Average			4.04		6.24		8.78		12.15	7.72	1.6

Table 10. HC emission concentration of cerium stearate additives.

RPM	F0	S20		S40		S60		S80		Average decline	Error (%)
	HC	HC	Decrement	HC	Decrement	HC	Decrement	HC	Decrement		
60%	85	84	1.18	82	3.53	78.5	7.65	78	8.24	5.15	1.4
70%	72.5	71	2.07	70	3.45	68.5	5.52	67	7.59	4.66	2.7
80%	58	57.5	0.86	55.1	5.00	54.3	6.38	52.8	8.97	5.30	1.8
90%	50	49.2	1.60	47	6.00	45.9	8.20	45.3	9.40	6.30	1.7
100%	48	47.5	1.04	46	4.17	44.5	7.29	43.6	9.17	5.42	1.4
Average			1.35		4.43		7.01		8.67	5.37	1.8

additives, the maximum reduction of CO concentration is 13.41%.

As can be seen from Fig. 17 and Table 10, with the increase of diesel engine speed, HC concentration discharged presents a downward trend. After comparative analysis, HC emission reduction effect also increases with the increase of the mass fraction of additives, and the maximum reduction of HC concentration is 9.40%.

As can be seen from Fig. 18 and Table 11, with the increase of diesel engine speed, the exhaust PM concentration shows an upward trend. After comparative analysis, the increase rate of PM emission increases with the increase of the mass fraction of additives, and the maximum increase of PM concentration is 12.18%.

It can be seen that the cerium stearate powder is analyzed by BET, SEM, XRD and EDS, and the comprehensive characterization data are obtained through the performance characterization. SEM images show that cerium stearate has irregular structure like round and massive particles, but no obvious agglomeration phenomenon is found, and the dispersion is good. However, through XRD analysis, it is found that there is a certain small intensity diffraction peak. Combination with X-ray energy spectrum analysis, it is found that there is impurity nitrogen element, but the impurity content was small, and the weight ratio

Table 11. PM emission concentration of cerium stearate additives.

RPM	F0	S20		S40		S60		S80		Average growth	Error (%)
	PM	PM	Growth	PM	Growth	PM	Growth	PM	Growth		
60%	580	588	1.38	603	3.97	617	6.38	620	6.90	4.66	2.1
70%	615	628.5	2.20	630	2.44	660	7.32	670	8.94	5.23	2.0
80%	645	664	2.95	687	3.46	701	8.68	716	11.01	6.53	2.7
90%	730	743	1.78	782	7.12	801	9.73	815	11.64	7.57	1.7
100%	780	792	1.54	820	5.13	830	6.41	875	12.18	6.32	1.9
Average			1.97		4.42		7.70		10.13	6.06	2.1

Table 12. Comparison of emission reduction effect.

		$Ce_2(CO_3)_3$	$Ce(C_{18}H_{35}O_2)_3$
NO_X	Maximum reduction rate	11.37	10.19
	Average reduction rate	7.29	5.63
CO	Maximum reduction rate	14.63	12.15
	Average reduction rate	8.99	7.72
HC	Maximum reduction rate	13.80	9.40
	Average reduction rate	8.39	5.37
PM	Maximum growth rate	10.86	12.18
	Average growth rate	5.53	6.06

was only 3.79%. The reason for the occurrence of impurities can be caused by dropping too much cerium nitrate solution into stearic acid solution during sample configuration. So the final prepared cerium stearate powder has cerium nitrate residue. After calculation and analysis, the specific surface area of cerium stearate powder is 11.7797m²/g, and the average pore size between powder particles is 32.9169 nm. Good emission reduction effect was obtained on the experimental platform, it is concluded that the emission concentration of NO_X, CO and HC decreases by 10.19%, 12.15% and 9.40% respectively, but the maximum increase of PM particle concentration is 12.18%. Therefore, compared with 0# diesel alone, the comprehensive consideration of cerium stearate fuel additives has a certain pollution reduction effect.

According to the above emission reduction experiments of cerium carbonate and cerium stearate fuel additives, Table 12 can be summarized for comparative analysis. As can be seen from Table 12, the reduction of NO_X, CO and HC emissions of cerium carbonate fuel additives is greater than that of cerium stearate, while the increase of PM emissions of cerium carbonate fuel additives is less than that of cerium stearate. Therefore, according to the emission reduction experiment, it can be concluded that the emission reduction effect of cerium carbonate fuel additives is better than cerium stearate.

Conclusions

From the emission reduction experiments of cerium carbonate and cerium stearate additives, it can be known that the emission reduction effect of cerium carbonate fuel additives is better than cerium stearate. Combined with the performance characterization data of two fuel additives, the specific surface area of cerium carbonate powder is greater than that of cerium stearate powder. Theoretically, the larger the specific surface area of powder is, the stronger the surface effect is, such as catalytic capacity, surface activity and surface adsorption capacity. Therefore, the emission reduction experiment in this paper is consistent with the theoretical data. Although cerium carbonate and cerium stearate studied in this paper belong to inorganic acid rare earth and organic acid rare earth respectively, it cannot simply be said that inorganic acid rare earth has better emission reduction performance than organic acid rare earth, so further research is needed.

The advantage of this paper is the first study for emission reduction performance of inorganic acid cerium and organic acid cerium by the combination of performance characterization and experimental, and the final conclusion is very consistent with the two way. The shortcoming is that only cerium carbonate and cerium stearate are used to represent inorganic cerium

and organic cerium respectively, which need to be further studied in the future.

Acknowledgments

In writing this paper, I have benefited from the presence of my colleagues. They generously helped me collect the materials and offered many invaluable suggestions. I hereby extend my grateful thanks to them for their kind help, without which the paper would not have been what it is.

Conflicts of Interest

The author declares that there is no conflict of interest regarding the publication of this paper.

Funding Statement

This work was supported by the National Natural Science Foundation of China. Grant number is 11272213.

References

1. PRELEC Z., MRAKOVCIC T., DRAGICEVIC V. Performance study of fuel oil additives in real power plant operating conditions. Fuel processing technology, **110**, 176, **2013**.
2. BENK A., COBAN A. A simple method for the production of fuel and fuel additives from renewable low-viscosity mineral oils (Number-10 oil) and their mixtures. Renewable energy, **147**, 1491, **2020**.
3. KIM D.C., KIM J.H., WOO J.K., SHIN D.H., LEE Y.S., KAUSHIK R.D . A new iron-nanofluid as fuel additive for particulate matter reduction in heavy fuel oil-fired boiler facility. Asian journal of chemistry, **20** (7), 5767, **2008**.
4. TUMANYAN B.P., SHCHERBAKOV P.Y., SHARIN E.A., MATIN M.E., MATVEEVA O.A. Effectiveness of Vegetable-Oil Fatty Acids as Antiwear Additives for Diesel Oils. Chemistry and technology of fuels and oils, **56** (4), 517, **2020**.
5. KHIDR T.T. The Effect of Commercial Additives as Pour Point Depressants for Fuel Oils. Petroleum science and technology, **33** (9), 975, **2015**.
6. SHAH P.R., GANESH A. A comparative study on influence of fuel additives with edible and non-edible vegetable oil based on fuel characterization and engine characteristics of diesel engine. Applied thermal engineering, **102**, 800, **2016**.
7. DANIOV A.M. A New Look at Fuel Additives. Petroleum chemistry, **60** (2), 147, **2020**.
8. JANG S.H., CHOI J.H. Comparison of fuel consumption and emission characteristics of various marine heavy fuel additives. Applied energy, **179**, 36, **2016**.
9. JAMIL A. A novel study of tungsten oxide nanocrystallites as fuel additive for diesel oil. Journal of TAIBAH university for science, **15** (1), 248, **2021**.
10. KADAROHMAN A., HERNANI, KHOERUNISA F., ASTUTI R.M. A potential study on clove oil, eugenol and eugenyl acetate as diesel fuel bio-additives and their performance on one cylinder engine. Transport, **25** (1), 66, **2010**.
11. AGAEV S.G., YAKOVLEV N.S. Influence of oil-soluble additives on dielectric properties of diesel fuel. Petroleum chemistry, **57** (3), 267, **2017**.
12. SHEVCHENKO E.B., SUKHANBERLIEV A.I., ABBASOV M.M., DANILOV A.M. Fatty acids of vegetable oils as components of anti-wear diesel-fuel Additives. Russian journal of applied chemistry, **92** (1), 166, **2019**.
13. SAIDAKHMEDOV A.I., KARPOV S.A., KAPUSTIN V.M. Effect of cottonseed oil additives and etherification products on diesel fuel properties. Chemistry and technology of fuels and oils, **47** (5), 331, **2011**.
14. DANILOV A.M. Development and use of fuel additives during 2006-2010. Chemistry and technology of fuels and oils, **47** (6), 470, **2012**.
15. AFSHAR E.A., TARIGHI S. The influence of temperature and catalyst additives on catalytic cracking of a heavy fuel oil. Petroleum science and technology, **33** (4), 415, **2015**.
16. FARAZMAND S., EHSANI M.R., SHADMAN M.M., AHMADI S., VEISI S., ABDI E. The effects of additives on the reduction of the pour point of diesel fuel and fuel oil. Petroleum science and technology, **34** (17), 1542, **2016**.
17. LARSSON E., OLANDER P., JACOBSON S. Boric acid as fuel additive - Friction experiments and reflections around its effect on fuel saving. Tribology international, **128**, 302, **2018**.
18. KIM D.C., SONG K.C., KAUSHK R.D. Fuel additives for particulate matter/dust reduction. Asian journal of chemistry, **20** (8), 5797, **2008**.
19. SUBRAMANIAN T., VARUVEL E.G., GANAPATHY, S., VEDHARAJ S., VALLINAYAGAM R. Role of fuel additives on reduction of NO_X emission from a diesel engine powered by camphor oil biofuel. Environmental science and pollution research, **25** (16), 15368, **2018**.
20. RYU Y., LEE Y., NAM J. Performance and emission characteristics of additives-enhanced heavy fuel oil in large two-stroke marine diesel engine. FUEL, **182**, 850, **2016**.
21. VALLBAUM E.T., MUONI R.T., SOONE J.H. Effect of a Shale Oil-Based Additive on the Properties of Biodiesel Fuel. Solid fuel chemistry, **52** (1), 44, **2018**.
22. LONDHE H., LUO G.Q., PARK S., KELLEY S.S., FANG T.G. Testing of anisole and methyl acetate as additives to diesel and biodiesel fuels in a compression ignition engine. FUEL, **246**, 79, **2019**.
23. DANILOV A.M. Research on fuel additives during 2011-2015. Chemistry and technology of fuels and oils, **53** (5), 705, **2017**.
24. AYNAZ M., DALIA A., MEHDI V., ABDOLLAH D., AMIR M. Synthesis of magnetic Fe_3O_4/activated carbon prepared from banana peel (BPAC@Fe_3O_4) and salvia seed (SSAC@Fe_3O_4) and applications in the adsorption of Basic Blue 41 textile dye from aqueous solutions. Applied Water Science, **12**, 88, **2022**.
25. RAZIEH K., FARID N., MOHAMMAD S., MOHAMAD J.S., SAEEDEH P., ABDOLLAH D., KIOMARS S., ALIREZA A. The association between air pollution and weather conditions with increase in the number of admissions of asthmatic patients in emergency wards: a case study in Kermanshah. Medical Journal of the Islamic Republic of Iran, **29**, 229, **2015**.

26. REZA S., ABDOLLAH D., ROYA A.G., HASAN Z.N., DARIUSH Z., MOHAMMAD M.M. Magnetic multi-walled carbon nanotube as effective adsorbent for ciprofloxacin (CIP) removal from aqueous solutions: Isotherm and Kinetics Studies. International Journal of Chemical Reactor Engineering, **10**, 1, **2019**.

27. ABDOLLAH D., MOHAMMAD R.S., AMIR S., MOHAMMAD M.M., HASAN Z.N. Statistical modeling of phenolic compounds adsorption onto low-cost adsorbent prepared from aloe vera leaves wastes using CCD-RSM optimization: effect of parameters, isotherm, and kinetic studies. Biomass Conversion and Biorefinery, **7**, 5, **2021**.